ORIGINAL PAPER

Hydrothermal process synthesized electrocatalytic multi-walled carbon nanotubes-inserted gold composite microparticles toward ethanol oxidation reaction

Keqiang Ding · Yahui Wang · Lu Liu ·
Likun Liu · Xi Zhang · Zhanhu Guo

Abstract Composite microparticles consisting of large gold (Au) particles embedded with multi-walled carbon nanotubes (MWCNTs), denoted as MWCNTs-Au, have been successfully prepared by a facile hydrothermal process of gold(III) chloride ($AuCl_3$) in a MWCNT aqueous solution. X-ray diffraction and scanning electron microscopy reveal that the obtained Au particles have an average diameter of about 500 nm and some MWCNTs are inserted into the Au particles. The MWCNTs-Au composites in the ethanol oxidation reaction (EOR) show quite different shape of cyclic voltammograms (CVs) toward EOR when compared to the previous CV reports on the pure Au substrate.

Keywords Hydrothermal · Composites · Au microparticles · Multi-walled carbon nanotubes · Ethanol oxidation reaction

1 Introduction

Due to their chemical stability, specific optical, and other physicochemical properties, gold (Au) nanoparticles are important objects of contemporary chemistry [1]. Au and its derivatives may be used as activators and catalysts for various systems, particularly in the cases where other noble metals such as palladium (Pd) and silver (Ag) including their colloids are undesirable [2]. Recently, the development of low temperature fuel cells, including proton exchange membrane fuel cells, direct methanol fuel cells, and direct ethanol fuel cells, has been intensively pursued due to their unique properties compared to the traditional batteries, such as their higher energy-conversion efficiency providing high-energy output with no harmful by-products [3, 4]. Hence, catalysts used for the oxygen reduction reaction, methanol oxidation reaction (MOR), and ethanol oxidation reaction (EOR), have been widely investigated. And noble metals, such as platinum (Pt) [5], Pd [6], and Au [7] nanoparticles have been intensively studied aiming to cut down the cost of producing fuel cells.

Till now, there are two typical methods for generating Au nanoparticles. The first is the chemical reduction reaction approach. For example, Seeber et al. [8] have addressed the Au/Pt bimetallic nanoparticle system, in which $NaAuCl_4$ $2H_2O$ and $NaBH_4$ were employed as the Au precursor and the reductive reagent, respectively. Tsakova et al. [9] have described the preparation of colloidal Au nanoparticles with $HAuCl_4$ and sodium citrate as the starting materials. The second is the electrochemical reduction reaction. For example, Yoshihara et al. [10] immobilized Au nanoparticles on the as-grown and oxygen-terminated (O-terminated) boron-doped diamond films electrochemically, in which the electrolyte solution was 0.1 M H_2SO_4 containing 0.3 mM $AuCl_4^-$ solution. To the best of our knowledge, the preparation of Au particles, including nano- and microparticles by a simple hydrothermal process has not been reported.

Meanwhile, carbon nanotubes (CNTs) have attracted a great deal of attention immediately after their reported by Iijima [11] due to their unique properties such as high

K. Ding (✉) · Y. Wang · L. Liu · L. Liu
College of Chemistry and Materials Science, Hebei Normal University, Shijiazhuang 050024, People's Republic of China
e-mail: dkeqiang@263.net

X. Zhang · Z. Guo (✉)
Integrated Composites Laboratory (ICL), Dan F. Smith Department of Chemical Engineering, Lamar University, Beaumont, TX 77710, USA
e-mail: zhanhu.guo@lamar.edu

specific surface area, large electrical conductivity, excellent mechanical properties [12]. Acting as an ideal substrate to modify the electrode surface was thought to be the main contribution of CNTs when used in the electrochemistry [13]. Thus, immobilizing metal nanoparticles on CNTs has turned into an interesting field mainly due to the key roles of CNTs and metal nanoparticles in the field of electrocatalysis, biosensors and so on [14].

Along with the development of nanoparticles, works on the preparation and applications of the microparticles have been widely proceeded. For example, Wang et al. [15] reported the electrodeposition of Pt microparticles on the surface of the nichrome matrix by cyclic voltammetry (CV) in an electrolyte solution containing 5 mM K_2PtCl_6 and 0.5 M H_2SO_4. Zhang et al. [16] addressed that self-assembly of the oleamide derivatives in ethanol/water solution can yield microspheres via a gradual temperature reduction and solvent volatilization process. Rosenzweig et al. [17] stated that Au nanoparticles can be covalently attached to the quantum dots-carboxyl-modified polystyrene surface to form composite microspheres, which can be used as fluorescence resonance energy transfer probes.

In this work, unique huge Au composite particles with multi-walled carbon nanotubes (MWCNTs) were prepared through a very simple hydrothermal process, in which no other reducing reagents were introduced except the MWCNTs and distilled water. X-ray diffraction (XRD), scanning electron microscopy (SEM), and energy dispersive X-ray spectroscopy were employed to characterize the composites particles. The electrocatalytic activities of these Au/MWCNTs composite particles toward EOR were evaluated by CV in a 1 M KOH solution.

2 Material and methods

2.1 Reagents and materials

MWCNTs (purity >95 %) of 10–20 nm diameter were purchased from Shenzhen nanotech port Co., Ltd. (China). All the electrodes were obtained from Tianjin Aida Co., Ltd (China). Deionized water was used to prepare the solutions. All the other chemicals were analytical grade and were used without any further purification.

2.2 Preparation of MWCNTs-inserted Au particles

The Au/MWCNTs composite particles were synthesized by a simple hydrothermal process as follows. First, 4 mL $AuCl_3 \cdot HCl \cdot 4H_2O$ (5×10^{-3} M) and 10 mg MWCNTs were mixed to yield a suspended solution, which was then ultrasonicated for 30 min. Second, the suspension was placed in a homemade autoclave at room temperature, and then the well-sealed autoclave was transferred to a box-type furnace.

Last, the temperature of the box-type furnace was increased to 200 °C within 20 min, and was kept at that temperature for various periods to complete the hydrothermal process. The hydrothermal process was implemented in a SRJX-8-13 box-type furnace equipped with a KSY 12–16 furnace temperature controller. The filtered samples were thoroughly washed with distilled water, and then dried in ambient conditions to obtain the MWCNTs-inserted Au particles (or called MWCNT-Au composites, denoted as MWCNTs-Au).

2.3 Preparation of MWCNTs-Au-coated electrode

Prior to each experiment, the working graphite electrode with a diameter of 3 mm was successively polished with 1 and 0.06 µm alumina powders on a microcloth wetted with doubly distilled water. This produced an electrode with a mirror-like surface. For the preparation of a MWCNTs-Au-coated electrode, 4.6 mg MWCNTs-Au composite material was added to a 1 mL ethanol solution of Nafion (the content of Nafion is 0.5 wt%), and then the mixture was treated for 30 min with ultrasonication to form a uniform suspension. The obtained suspension (5 µL) was dropped on the surface of a well-treated graphite electrode. Finally, the resultant MWCNTs-Au-modified graphite electrode was dried with hot air at room temperature.

2.4 Characterization

The XRD analysis of the catalyst was carried out on a Bruker D8 ADVANCE X-ray diffractometer equipped with a Cu Kα source ($\lambda = 0.154$ nm) at 40 kV and 30 mA. The 2θ angular region between 20 and 80° was explored at a scan rate of 1°/step. The samples obtained were characterized using SEM (S-4800, HITACHI, Japan). EDX spectrum analysis was carried out on an X-ray energy instrument (EDAX, PV-9900, USA).

The electrochemical experiments were conducted on a model CHI660B electrochemical working station (Chenhua, Shanghai, China). A conventional three-electrode system was employed, in which a MWCNTs-Au-modified graphite electrode and platinum wire were used as the working electrode and counter electrode, respectively. The reference electrode was a saturated calomel electrode (SCE). All the potentials in this paper are reported with respect to SCE. Experiments were carried out at room temperature.

3 Results and discussion

3.1 XRD analysis

The typical XRD patterns of the samples obtained are shown in Fig. 1. For pattern **b** in Fig. 1, the diffraction

peaks at 2θ of 26.1° was indexed to the (002) planes of CNTs (JCPDS card: 26-1077), which is consistent with the previous report [18]. After the hydrothermal process, the diffraction peaks corresponding to CNTs were still clearly observed, suggesting that the hydrothermal process did not destroy the crystal structure of the MWCNTs. Also, some new peaks were observed at 38, 45, 65, 78, and 82°, pattern **a**, which correspond to the characteristic (111), (200), (220), (311), and (222) planes of single face-centered cubic structural Au (00-002-1095), Fig. 1c. This is consistent with the former report [19] very well. Since no other diffraction peaks were observed, Fig. 1 strongly demonstrates that Au particles have been successfully formed on the surface of the MWCNTs. The average crystallite size was estimated using the Debye-Scherer formula, $t = 0.89\lambda/(\beta\cos\theta_B)$ [20], where λ is the X-ray wavelength (1.54 Å), θ_B is the Bragg diffraction angle, and β is the peak width at half-maximum. Based on this formula, for the (111) and (200) peak, the average crystallite size of Au particles was estimated to be 7.1 and 8.3 nm, respectively. Unfortunately, these calculated sizes were rather smaller than those observed by SEM images, Fig. 3, indicating that the Au composite particles are made of small crystals.

3.2 SEM and EDX characterization

The samples of MWCNTs-inserted Au composite particles were also analyzed by SEM and EDX. Figure 2 shows the EDX spectra of the MWCNTs-inserted Au particles (as shown by line **a**), in which no other peaks were observed except the Au and C elemental peaks, implying that only Au particles were formed by this simple hydrothermal process, which is consistent with the results obtained from
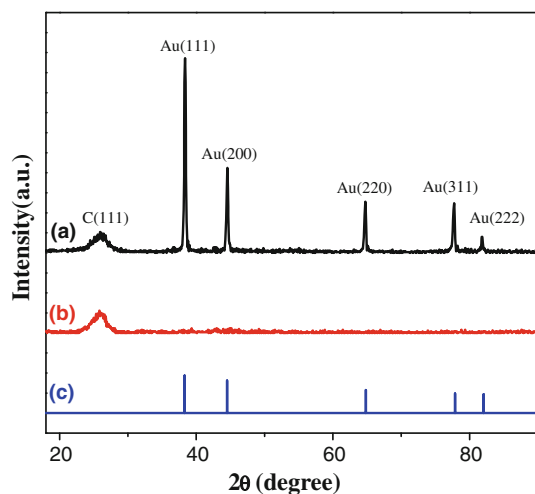
XRD analysis, Fig. 1. The EDX spectrum [6] also shows that the wt% of C and Au for the precursors containing $AuCl_3 \cdot HCl \cdot 4H_2O$ and MWCNTs were 79.4 and 3.3 wt%, respectively. While after the hydrothermal process, the wt% of C and Au sample were varied to be 76.6 and 18.2 wt%, respectively. That is to say, in the hydrothermal process, carbon was consumed, and more Au was generated. Due to its simplicity, this technique may be feasible for the usage in industrial production.

The SEM images are shown in Fig. 3a Obviously, no substances were found on the surface of MWCNTs, Fig. 3a. While after 2-h hydrothermal process, large Au particles were observed, many protuberances were also observed on the surface of these particles. More interestingly, as illustrated by the circled part in image Fig. 3b, huge the Au particles were embedded with MWCNTs. The average diameter of the obtained particle was around 500 nm, larger than the crystallite size calculated from the XRD patterns, Fig. 1, indicating that the composite particles are made of small Au crystals. Moreover, the morphologies of MWCNTs were preserved very well even after the hydrothermal process, suggesting that the hydrothermal process did not destroy the crystal structure of MWCNTs and is consistent with the XRD observation Fig. 1.

Lu et al. [21] have reported the preparation of Au nanoparticles, in which $HAuCl_4 \cdot 3H_2O$ and $NaBH_4$ were employed as the Au precursor and reducing reagent, respectively. Li et al. [22] have reported the synthesis of Au nanoparticles, using cacumen platycladi leaf as the reducing agent. Thus, there must be a reductive reagent to reduce Au^{3+} to yield Au atoms, leading to the formation of Au particles. What is the reductive reagent in the above hydrothermal process and how do we explain the hydrothermal process? Numerous attempts confirmed that Au
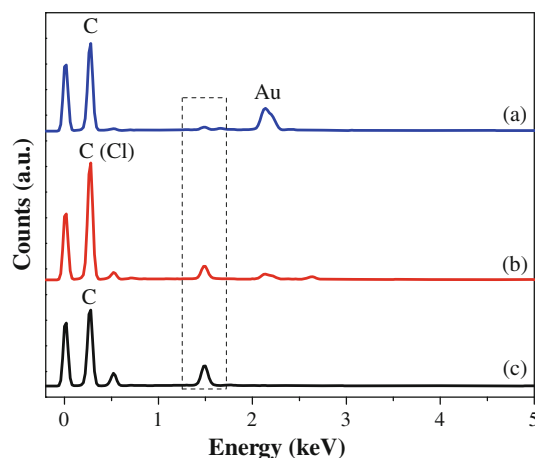

Fig. 1 XRD patterns for the samples. (*a*) MWCNTs/Au sample prepared by the hydrothermal process for 2 h, (*b*) pure MWCNTs, and (*c*) the standard XRD pattern for pure gold

Fig. 2 EDX spectra for (*a*) the sample after hydrothermal process for 2 h, (*b*) the precursors before the reaction, and (*c*) pure MWCNTs
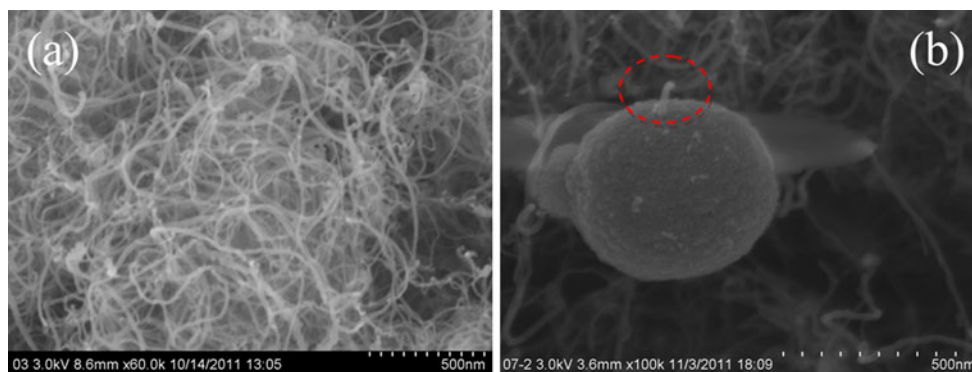
Fig. 3 SEM images for **a** pure MWCNTs and **b** the obtained MWCNTs-inserted Au composite particles prepared by hydrothermal process for 2 h

particles could not be fabricated by this hydrothermal process in the absence of MWCNTs and thus it is concluded that MWCNTs served as the reducing reagent in the above hydrothermal process.

The digital photos of the aqueous $AuCl_3$ solution used in the hydrothermal process are displayed in the inset of Fig. 4. A red-yellow solution was observed, Fig. 4a, when $AuCl_3$ was dissolved in distilled water, While, after hydrothermal process, a colorless solution was observed after MWCNTs were filtered, indicating that some reactions took place between the Au^{3+} solution and the introduced MWCNTs. Fig. 4 shows the ultraviolet–visible (UV–Vis) spectra for the above two solutions. The solution having $AuCl_3$ is observed to have two absorption peaks at around 225 and 290 nm, respectively, which is consistent with the previous report [21]. Lu et al. [21] proposed that the shoulder peak at around 290 nm could be assigned to the ligand-to-metal charge-transition, indicative of the formation of complexes like $[AuCl_4]^-$. Thus, in this case, Au^{3+} in the as-prepared solution should exists in the form of $[AuCl_4]^-$, rather than Au^{3+}. While after the reaction, a colorless solution was obtained. It indicated that all the $[AuCl_4]^-$ were totally consumed or reduced by the introduced MWCNTs, since the color of the Au^{3+} aqueous solution cannot be altered by the hydrothermal process in the absence of MWCNTs. In general, due to the self-oxidation, the carbon surface is usually decorated with oxygen-containing functional groups, from compounds such as carboxylic acids, phenols, lactones, carboxylic anhydrates, ketones, ethers, quinones, or pyrones [23]. Therefore, in such a sealed autoclave at 200 °C and under a higher pressure, the $[AuCl_4]^-$ was easily reduced to yield Au atoms by some organic groups that were attached to the surface of the MWCNTs.

A close inspection revealed that after ultrasonication, some nanoparticles with a diameter of around 150 nm and well-defined crystal structure were observed in the mixture containing $AuCl_3$ and MWCNTs, as shown by the green-circled part in Fig. 5. The localized EDX spectra indicated that these nanoparticles have only element of Au, and those layered particles circled by red line in Fig. 5 have only two elements, i.e., Cl and Au (data no shown here). That is to say, the small regular particles circled by green line in Fig. 5 are Au particles, and the irregular layered particles are the starting materials of $AuCl_3$ as opposed to other substances. How are these Au particles formed? EDX spectra, as shown by the circled part in Fig. 2, revealed that small amount of Al were contained by MWCNTs [24]. One can see from Fig. 2 that after ultrasonication, for the precursors containing $AuCl_3$ and MWCNT, as shown by the square-dashed part, the intensity of peak corresponding to Al in line **b** was greatly lowered compared to the pure MWCNTs (line **c**). The weight percentage measurement also indicated that after the hydrothermal process, the weight percentage of Al varied from 2.23 wt% in pure MWCNTs to 0.34 wt% in the precursors. Thus, under the ultrasonication condition, the left Al reacted with Au^{3+} to generate Au atoms by a chemical redox reaction as
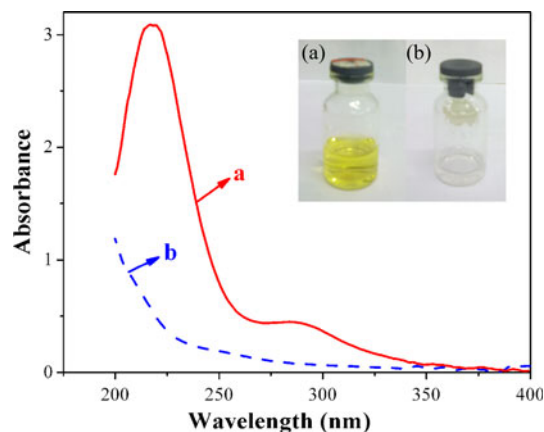

Fig. 4 UV spectra for (**a**) the solution containing Au^{3+}, (**b**) for the solution obtained after hydrothermal process for 2 h. *Inset* digital photos for solutions. Photo *a* solution containing Au^{3+}; photo *b* solution after 2-h reaction

$Au^{3+} + Al = Au + Al^{3+}$. Meanwhile, the MWCNTs served as a reducing agent [25] to react with Au^{3+} to form Au atoms, which are then nucleated and grown to form Au nanoparticles on the CNTs.

But how to understand the formation process of MWCNTs-inserted Au composite particles? There are many defects on the surface of CNTs according to the former reports [13, 26], thus these CNTs having defects can serve as the nucleating sites for the formed Au atoms, which are easily nucleated on the surface of CNTs during the chemical redox reaction between Au^{3+} and the doped metal such as Al or CNTs, as shown schematically by the step **1** in Fig. 6. And then, due to the conductive nature of the CNTs, the newly formed Au atoms have a trend to grow on the nuclei of Au nucleated around the CNTs (as shown by step **2** and **3** in Fig. 6), as a result the MWCNTs-inserted Au microparticles were fabricated (as shown by step **4** in Fig. 6). These MWCNTs-inserted Au composite particles have great potential be used as the specific conductor in designing microdevices [27, 28].

3.3 Electrocatalysis of MWCNTs-Au composite microparticle toward EOR

Although the quantitative information is not easily acquired by CV, CV can describe electrochemical reactions directly. Seeber et al. [8] have presented the CVs of MOR measured on an Au nanoparticle modified glassy carbon electrode, in which a pair of normal redox peaks was observed. Strbac et al. [29] have also demonstrated the CVs of EOR on Au (111) in 0.5 M H_2SO_4, where a pair of abnormal redox peaks was displayed. Except for the work reported by Lamy et al. [30] and Varela [31], to the best of
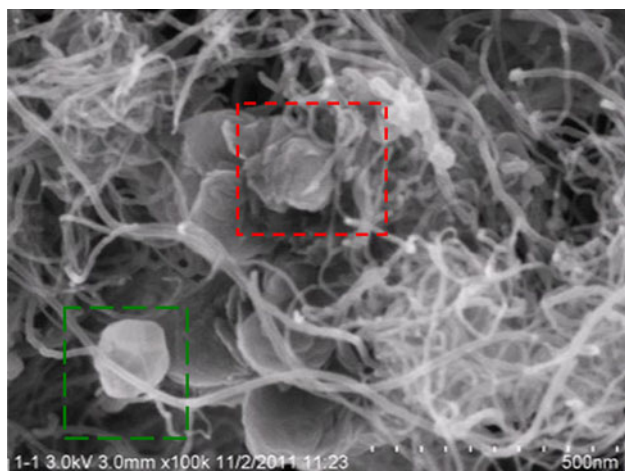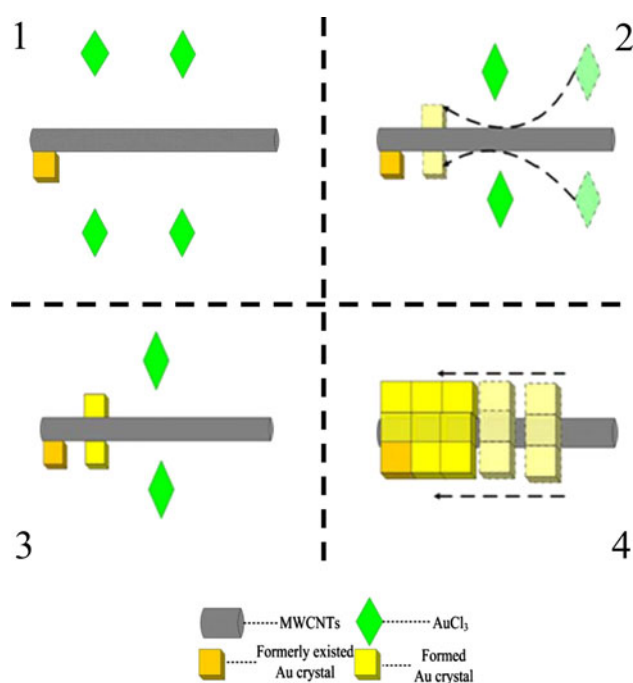

Fig. 6 Proposed formation scheme of Au composite particles inserted with MWCNTs by a hydrothermal process in the presence of MWCNTs. Step 1: Au nucleated on the MWCNTs; step 2 and step 3: the growth of the newly formed Au single crystals along the tube of MWCNTs; step 4: the formed MWCNTs-inserted Au composite particle

our knowledge, CVs of EOR in alkaline solution on Au-modified electrode have been rarely reported.

Here, the CVs of EOR in alkaline solution on the MWCNTs-Au composite particles modified graphite electrode are shown in Fig. 7. As shown by the blue curves, no oxidation peaks can be displayed on the MWCNTs-modified graphite electrode, but under the same conditions, the CVs for EOR were observed on the MWCNTs-Au composite particles-coated graphite electrode. Two oxidation peaks, respectively, located at around 0.11 V in the forward potential scan (Peak **f**) and at −0.02 V in the backward potential scan (Peak **b**), are displayed clearly. This result strongly demonstrated that EOR in the alkaline solution took place on the surface of Au particles instead of on the MWCNTs-modified electrode. The shape of CVs for EOR, Fig. 7, is very similar to that of CVs of EOR on Au substrate [29]. However, the CVs of the EOR [29] were obtained in 0.5 M H_2SO_4 rather than in an alkaline solution. Lamy et al. [30] displayed the CVs of EOR that was recorded on Au electrode in a 0.1 M NaOH, where a pair of normal redox peaks corresponding to EOR was exhibited, no anomalous oxidation peak in the negative-direction potential scan was observed. That is to say, the shape of the CVs for EOR shown here is rather different from that of the previously reported ones.

Fig. 5 SEM images for the precursors containing $AuCl_3$ and MWCNTs. *Green-circled* part: pure Au particles; *red-circled* part: $AuCl_3$ particles. (Color figure online)

Figure 8 shows a series of CV curves obtained at various scan rates. As shown by the red line, in the absence of ethanol, no peaks can be observed on the MWCNTs-Au composite particles modified graphite electrode. While in the presence of ethanol, the CVs of EOR are clearly displayed. It suggested that the oxidation peaks were due to the introduced ethanol rather than other substances. The oxidation peak currents for both Peak **f** and **b** are linear to the square root of scan rates, the inset in Fig. 8, indicating that the process of EOR on the modified electrode was determined by a diffusion-controlled process [32].

Actually, the mechanism of EOR on Au electrode in alkaline solution remains unclear. For instance, Lamy et al. [30] have demonstrated by Fourier transform infrared (FT-IR) spectroscopy that acetate is the only detectable product of EOR in alkaline solution via the following reaction,

i.e., $CH_3\text{-}CH_2OH + 4OH^- \rightarrow CH_3\text{-}COOH + 3H_2O + 4e^-$, and they proposed that during the positive-direction potential scan, Au oxide will form, and in the negative-direction potential scan, the oxidation of ethanol will be accompanied by the reduction of Au oxide on the surface of Au electrode. Recently, Attard et. al. [33] reported the cyclic voltammetric behavior of EOR in alkaline medium on the gold attached on Pt{hkl} electrodes and pointed out that the EOR in alkaline medium is very structure sensitive for submonolayer gold coverage. In other words, the EOR on Au in alkaline solution can be easily affected by the microcrystal structure of the gold electrode used. Since the shape of CVs for EOR shown in Fig. 7 is very similar to the formerly reported CVs of the EOR on Pd substrate [6], the mechanism of EOR on Au is analogous to that occurring on Pd substrate. That is, the OH^- ions are first chemisorbed in the initial stage of the oxide formation and
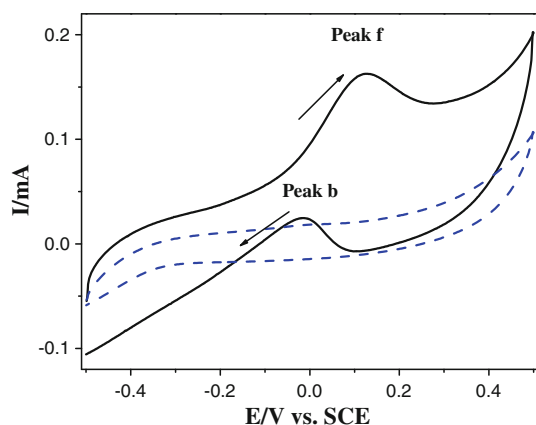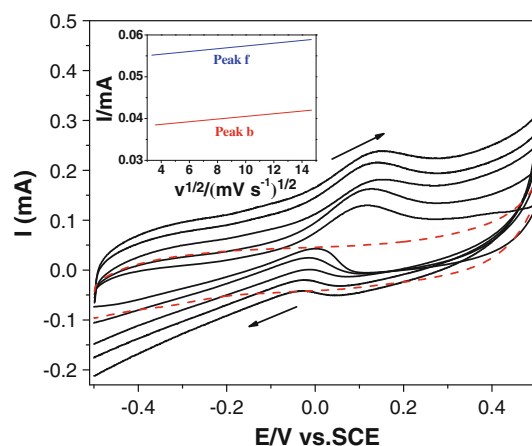

Fig. 8 Cyclic voltammograms (CVs) for ethanol oxidation reaction (EOR) obtained on the MWCNTs-Au composite particles-coated graphite electrode in 1 M KOH solution containing 1 M ethanol. The *red line* was obtained at 50 mV s^{-1} in the absence of ethanol. From down to up, the scan rates are 20, 50, 100, 150, and 200 mV s^{-1}, respectively. (Color figure online)

then they are transformed into higher valence oxides at higher potentials [34, 35]. In other words, in the positive-direction potential scan, Au_2O (or Au_2O_3) was formed, which covered on some active sites of Au surface and hindered the oxidation of ethanol. And, in the negative-going potential sweep, more Au active sites were released, on which EOR could still occur.

Evidently, the hydrothermal time employed has a strong influence on the morphology and size of the resultant Au particles, which can greatly affect the electrocatalysis toward EOR. As shown in Fig. 9b, the intensity of the diffraction peak corresponding to plane (111) is higher than that for the samples prepared by the hydrothermal process for 1 h, suggesting that the crystallinity of sample prepared for 2 h is higher than that prepared for 1 h. While for the sample prepared by hydrothermal process for 3 h, Fig. 9c, no evident change of the intensity of XRD pattern was found when compared to Fig. 9b. Different crystallinities of the resultant Au particles may result in different electrocatalysis toward EOR.

Chronoamperometry is a powerful technique to compare the electrocatalysis of various catalysts [36, 37]. Thus, the current–time curves were conducted at a potential of 0.13 V versus SCE. It can be seen that the steady-state current plateau, Fig. 10b for the Au composite particles prepared from 2-h hydrothermal process is the highest among the three samples. With increasing the hydrothermal process time, more Au particles were generated, leading to more active surfaces of Au particles for EOR, thus the electrocatalysis of the sample, Fig. 10b, is superior to the sample prepared by 1-h hydrothermal process. When the hydrothermal process time increases to 3 h, the active
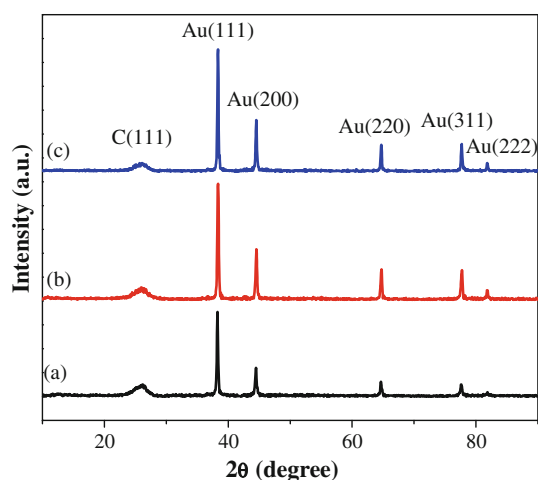

Fig. 7 CVs of EOR obtained at 50 mV s^{-1} on the MWCNTs-inserted Au composite particles supported on MWCNTs in 1 M KOH solution containing 1 M ethanol, and the *blue line* was measured on the MWCNTs-modified graphite electrode at 50 mV s^{-1}. (Color figure online)

Fig. 9 XRD patterns for the samples obtained by the hydrothermal reaction with a reaction time of (*a*) 1 h, (*b*) 2 h, and (*c*) 3 h

surface of Au particles was decreased due to the attachment of MWCNTs generating a lowered electrocatalysis toward EOR, Fig. 10c. Therefore, these current–time curves strongly demonstrate that the catalysis of the as-prepared Au composite particles toward EOR is closely related to the hydrothermal process time employed.

4 Conclusion

For the first time, Au composite particles embedded with MWCNTs were prepared with an average diameter of about 500 nm by a simple hydrothermal process of aqueous AuCl$_3$ solution in the presence of MWCNTs, in which no other reducing reagents were introduced. SEM strongly demonstrated the Au composites particles were inserted by the MWCNTs. Also the CVs of EOR indicated that the
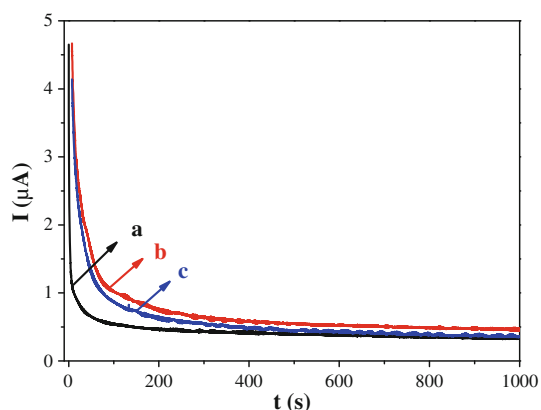
MWCNTs-Au composite particles have the capability for EOR in alkaline solution, in which the shape of CVs is rather different from the previously reported one. And, further work revealed that the electrocatalysis of the Au composite particles toward EOR is closely related to the hydrothermal process time employed. Except from exhibiting the CVs of EOR with different shapes compared to the previously published ones, these novel Au/MWCNTs composite particles, namely, MWCNTs-inserted Au composite microparticles, prepared from the facile one-step hydrothermal reaction are expected to be very helpful for the microdevices as well [38].

References

1. Lim B, Kobayashi H, Yu T, Wang J, Kim MJ, Li ZY, Rycenga M (2010) J Am Chem Soc 132:2506
2. Bu X, Yuan J, Song J, Han D, Niu L (2009) Mater Chem Phys 116:153
3. Jiang Q, Jiang L, Qi J, Wang S, Sun G (2011) Electrochim Acta 56:6431
4. Xu Z, Yu J, Liu G (2011) Electrochem Commun 13:1260
5. Tian N, Zhou ZY, Sun SG, Ding Y, Wang ZL (2007) Science 316:732
6. Ding K, Yang G, Wei S, Mavinakuli P, Guo Z (2010) Ind Eng Chem Res 4911:415
7. Jaramillo TF, Baeck SH, Cuenya BR, McFarland EW (2003) J Am Chem Soc 125:7148
8. Terzi F, Zanardi C, Daolio S, Fabrizio M, Seeber R (2011) Electrochim Acta 56:3673
9. Stoyanova A, Ivanov S, Tsakova V, Bund A (2011) Electrochim Acta 56:3693
10. Zhang Y, Suryanarayanan V, Nakazawa I, Yoshihara S, Shirakashi T (2004) Electrochim Acta 49:5235
11. Iijima S (1991) Nature 354:56
12. Davies TJ, Hyde ME, Compton RG (2005) Angew Chem Int Ed 44:5121
13. Ding KQ, Okajima T, Ohsaka T (2007) Electrochem 75:35
14. Hu L, Hecht DS, Grüner G (2010) Fabr Prop Appl 110:5790
15. Wang Z, Gao G, Zhu H, Sun Z, Liu H, Zhao X (2009) Int J Hydrogen Energy 34:9334
16. Zhang L, Jeong YI, Zheng S, Suh H, Kang DH, Kim I (2013) Langmuir. doi:10.1021/la303634y
17. Quach AD, Crivat G, Tarr MA, Rosenzweig Z (2011) J Am Chem Soc 133:2028
18. Xu J, Hua K, Sun G, Wang C, Lv X, Wang Y (2006) Electrochem Commun 8:982
19. Guerra-Balcázar M, Morales-Acosta D, Castaneda F, Ledesma-García J, Arriaga LG (2010) Electrochem Commun 12:864
20. Radmilovic V, Gasteiger HA, Ross PN (1995) J Catal 154:98
21. Bao C, Jin M, Lu R, Zhang T, Zhao Y (2003) Mater Chem Phys 82:812
22. Zhan G, Huang J, Du M, Abdul-Rauf I, Ma Y, Li Q (2011) Mater Lett 65:2989

Fig. 10 Chronoamperograms obtained at 0.13 V (vs. SCE) in 1 M KOH solution containing 1 M ethanol on MWCNTs-inserted Au composite particles modified graphite electrode, in which the hydrothermal process time used for preparing Au huge particles is *a* 1 h, *b* 2 h, and *c* 3 h

23. Hulicova-Jurcakova D, Seredych M, Lu GQ, Kodiweera NKAC, Stallworth PE, Greenbaum S, Bandosz TJ (2009) Carbon 47:1576
24. Banks CE, Crossley A, Salter C, Wilkins SJ, Compton RG (2006) Angew Chem Int Edit 45:2533
25. Gu H, Rapole S, Huang Y, Cao D, Luo Z, Wei S, Guo Z (2013) J Mater Chem. doi:10.1039/C2TA00550F
26. Banks CE, Davies TJ, Wildgoose GG, Compton RG (2005) Chem Commun 17:829
27. Schessler HM, Karpovich DS, Blanchard GJ (1996) J Am Chem Soc 118:9645
28. Farrer RA, LaFratta CN, Li L, Praino J, Naughton MJ, Saleh BEA, Teich MC, Fourkas JT (2006) J Am Chem Soc 128:1796
29. Strbac S, Avramov Ivic M (2009) Electrochim Acta 54:5408
30. Tremiliosi-Filho G, Gonzalez ER, Motheo AJ, Belgsir EM, Léger JM, Lamy C (1998) Electroanal Chem 444:31
31. de Lima RB, Varela H (2008) Gold Bull 41:15
32. Shi J, Ci P, Wang F, Peng H, Yang P, Wang L, Wang Q, Chu PK (2011) Electrochim Acta 56:4197
33. Hazzazi OA, Attard GA, Wells PB, Vidal-Iglesias FJ, Casadesus M (2009) J Electroanal Chem 625:123
34. Grden M, Czerwinski A (2008) J Solid State Electrochem 12:375
35. Grden M, Kotowski J, Czerwinski A (2000) J Solid State Electrochem 4:273
36. Sun ZP, Zhang XG, Liang YY, Li HL (2009) Electrochem Commun 11:557
37. Wang Q, Sun Z, Ding K (2010) J New Mater Electrochem Syst 13:119
38. Hoshino Y, Imamura K, Yue M, Inoue G, Miura Y (2012) J Am Chem Soc 134:18177